DOI: 10.1002/chem.200600892

Heavy-Metal-Ion Capture, Ion-Exchange, and Exceptional Acid Stability of the Open-Framework Chalcogenide $(NH_4)_4In_{12}Se_{20}$

Manolis J. Manos,[a] Christos D. Malliakas,[a] and Mercouri G. Kanatzidis*[a, b]

Abstract: The hydrothermal synthesis of the purely inorganic open-framework indium selenide $(NH_4)_4In_{12}Se_{20}$ (**1**) is reported. Compound **1** exhibits a unique three-dimensional open-framework structure. The framework of **1** shows an unusual, for a chalcogenide compound, rigidity arising from the unprecedented connection mode of its building blocks. Compound **1** possesses ion exchange capacity for Cs^+, Rb^+, NH_4^+, but it has selectivity against Na^+ and Li^+. It also showed exceptional stability in relatively concentrated hydrochloric acid. Ion exchange of **1** with hydrochloric water solutions can produce its solid acid analogue $H_2(NH_4)_2In_{12}Se_{20}$. The maximum cation-exchange capacity of **1** was found equal to two equivalents per mol, which is consistent with an exchange mechanism taking place in the 1D-channels formed by the largest cavities. In addition, **1** can do ion-exchange with heavy-metal ions like Hg^{2+}, Pb^{2+}, and Ag^+. The capacity of **1** to clean water solutions from heavy-metal ions was preliminarily investigated and found very high. Specifically, **1** can remove 99.9% of Hg^{2+}, 99.8% of Ag^+, and 94.9% of Pb^{2+} from aqueous solutions of each of these ions. Using different synthetic conditions, we isolated compound $(NH_4)_2In_{12}Se_{19}$ (**2**), which also has as good an acid stability as **1**, but no ion-exchange properties. Overall, this work provides new hydrothermal synthetic approaches for isolation of all-inorganic open-framework chalcogenides.

Keywords: chalcogens · indium · ion exchange · selenium · solid acid

Introduction

Chalcogenides with extended open frameworks can simultaneously possess zeolitic properties, such as solid acid and ion exchange. In addition, they can exhibit unique reactivity deriving from the nature of the framework and semiconductor properties that provide electronic, optical, and photonic phenomena. Such materials are typically synthesized with solid state or hydrothermal methods,[1–4] although there are examples isolated from room-temperature solution reactions.[2d] Generally, organic structure-directing agents are used and the reaction temperatures lie in the range of 150–200 °C.[2,3] Hydrothermal synthesis conditions (in the presence of organic amines) for open-framework chalcogenides above 200 °C have been not explored, although it is likely to result in decomposition of the organic templates and isolation of new frameworks, in which the counterions are simpler organic species or even purely inorganic such as NH_4^+.

Purely inorganic chalcogenides with open frameworks are relatively rare and the few examples reported so far revealed remarkable ion-exchange and fast ionic-conduction properties.[1k,l,3d,5,6] Moreover, the pore structure of purely inorganic phases is less likely to collapse on heating than that of organic-containing materials, as has been demonstrated in inorganic metal phosphates.[7]

Typical examples of hydrothermally synthesized open-framework chalcogenides are indium sulfides based on supertetrahedral (T_n) clusters as building blocks.[2,3] There are only a few reported examples of open-framework indium selenides.[8] They tend to adopt a variety of structural types[8a] and have narrower band gaps than the sulfides, which can make them promising for photocatalytic applications including solar hydrogen generation.[9]

[a] Dr. M. J. Manos, C. D. Malliakas, Prof. M. G. Kanatzidis
Department of Chemistry, Michigan Sate University
East Lansing MI 48842–1793 (USA)

[b] Prof. M. G. Kanatzidis
current address: Department of Chemistry
Northwestern University, 2145 Sheridan Rd
Evanston, IL 60208 (USA)
Fax: (+1) 847-491-1541
E-mail: m-kanatzidis@northwestern.edu

Supporting information for this article is available on the WWW under http://www.chemeurj.org/ or from the author. It contains crystallographic information files (CIF) for compounds **1** and **2** as well as representations of the structure of compound **2** and the solid-state UV/Vis reflectance spectra for the Ag, Hg, and Pb exchanged materials.

Herein, we describe the purely inorganic open-framework compounds $(NH_4)_4In_{12}Se_{20}$ (**1**) and $(NH_4)_2In_{12}Se_{19}$ (**2**), which to the best of our knowledge are not built on any known clusters. The unique structure type of compound **1** exhibits facile ion-exchange properties with a series of cations that are reminiscent to those of small pore zeolites. The chalcogenide framework has innate reactivity towards soft heavy-metal ions (Hg^{2+}, Pb^{2+}, Ag^{+}) and its pores are well suited for their capture. We show that **1** can effectively and selectively remove such metal ions from water. The capacity of **1** for heavy-metal-ion remediation is well comparable to that of the mesoporous thiol-functionalized silicates, known as the most efficient materials for the removal of heavy-metal ions from aqueous solutions.[10] Compound **2** is isostructural to $K_2In_{12}Se_{19}$.[11] It has a much less open framework that does not favor ion-exchange chemistry. Both **1** and **2** are extremely stable in highly acidic environment ($pH \approx 0$), in which many metal chalcogenides cannot survive.[12] Consequently, a stable, solid chalcogenide acid can be produced by the treatment of **1** with strong acidic solutions.

Results and Discussion

Synthesis of compounds 1 and 2: Compound $(NH_4)_4In_{12}Se_{20}$ (**1**) was initially isolated in the form of red rodlike crystals (Figure 1a) from a three-week hydrothermal reaction of In, Se, and DPA (dipropylamine) at 190 °C. These conditions resulted in decomposition of the organic amine to NH_4^+. The discovery of NH_4^+ in the structure led to a more rational synthesis of **1** by using shorter (24–48 h) hydrothermal reactions at 250 °C in concentrated NH_4OH (28–30 % in H_2O) as solvent with no additional water or organic amine. Interestingly, 24 h hydrothermal reactions of In and Se at 250 °C with dilute aqueous solutions of NH_4OH or the use of water and various organic amines always resulted in isolation of different compound $(NH_4)_2In_{12}Se_{19}$ (**2**) in the form of polyhedral-shape crystals, Figure 1b.

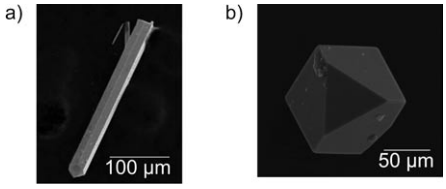

Figure 1. a) Scanning electron microscopy (SEM) image of a rod-shaped crystal of **1**; b) SEM image of a crystal of **2** with a polyhedral shape.

There are only two other types of In-Se open-framework compounds reported prior to this work, namely: the $[In_{10}Se_{18}]^{6-}$ and $[In_{33}Se_{56}]^{13-}$.[8] These were synthesized using temperatures near 200 °C and reaction times of 6–7 days. These are milder reaction conditions than those employed in the current work and this likely was the main reason that the organic amines used as structure-directing agents in the synthesis of these compounds remained intact. The reaction conditions, however, may not be the only factor affecting the decomposition of organic amines to NH_4^+, since such decomposition has been observed in metal phosphates under relatively mild conditions (200 °C, 4 days reactions).[13] The frameworks of $[In_{33}Se_{56}]^{13-}$ and $[In_{10}Se_{18}]^{6-}$ hosting large organic cations are much more open (accessible volumes $\approx 50\,\%$) than the framework of **1** (accessible volume $\approx 27\,\%$) hosting the small NH_4^+ ions. When the same hydrothermal reaction of In, Se, and organic amine was conducted at 250 °C for 1–2 days, it led to isolation of compound **2** with a much smaller accessible volume at $\approx 18\,\%$. Both compounds **1** and **2** host ammonium ions in their cavities. Thus, in this case the factor affecting the openness of the structure is presumably the reaction temperature (and not the size of the counterion); the higher the reaction temperature, the denser the phase formed. The exception to this rule is the isolation of compound **1** at 250 °C in a concentrated aqueous solution of NH_4OH. Remarkably, under such synthetic conditions, compound **2** could not be observed. The reaction paths for isolation of compounds **1** and **2** as well as of the $[In_{33}Se_{56}]^{13-}$ and $[In_{10}Se_{18}]^{6-}$ frameworks are summarized in Scheme 1.

To the best of our knowledge, the use of concentrated NH_4OH as a solvent in the synthesis of complex chalcogenides has not been reported prior to this work. Due to the extremely alkaline conditions and the very high NH_4^+ con-

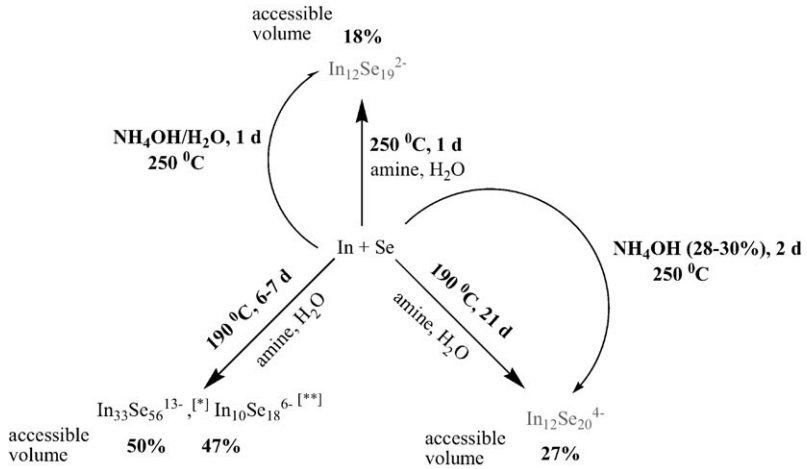

[*] From reference [5b]; [**] From reference [5a]

Scheme 1. Synthetic routes leading to the isolation of compounds **1**, **2**, and the known $[In_{33}Se_{56}]^{13-}$ and $[In_{10}Se_{18}]^{6-}$ materials.

centration, such an unusual solvent can be unique in stabilizing novel compounds.

Crystal structures of 1 and 2: Compound **1** crystallizes in the noncentrosymmetric orthorhombic space group $Pca2_1$. The structure of **1** seems to be based on nona-nuclear clusters $[In_9(\mu_3\text{-}Se)_4(\mu_2\text{-}Se)_6Se_{5\times1/2}Se_{5\times1/3}]$ (**1a**) built up by the interconnection of trinuclear $[In_3Se(Se_{1/2})_6(Se_{1/3})_3]$ and binuclear $[In_2Se_{1/3}(Se_{1/2})_6]$ units, Figure 2a. The trinuclear units are formed by three $InSe_4$ tetrahedra with a common corner (Se17 or the Se9/Se9 A split site). The binuclear moieties are constructed from two $InSe_4$ tetrahedra also with a common corner. The In–Se distances lie in the range of 2.503(4)–2.654(3) Å. The bond lengths of In atoms with the Se9A (one of the Se atoms of the split site) range from 2.600(19) to 2.727(19) Å. The nona-nuclear clusters stack to form columns running along the *a* axis, Figures 2b and 3. In these columns, the clusters are connected to each other by sharing corners between their binuclear $[In_2Se_{1/3}(Se_{1/2})_6]$ moieties, Figure 2c. Alternatively, each column may be viewed as three chains of corner-sharing $InSe_4$ tetrahedra, running along the *a* axis, that are bridged through the trinuclear $[In_3Se(Se_{1/2})_6(Se_{1/3})_3]$ units, Figure 2c.

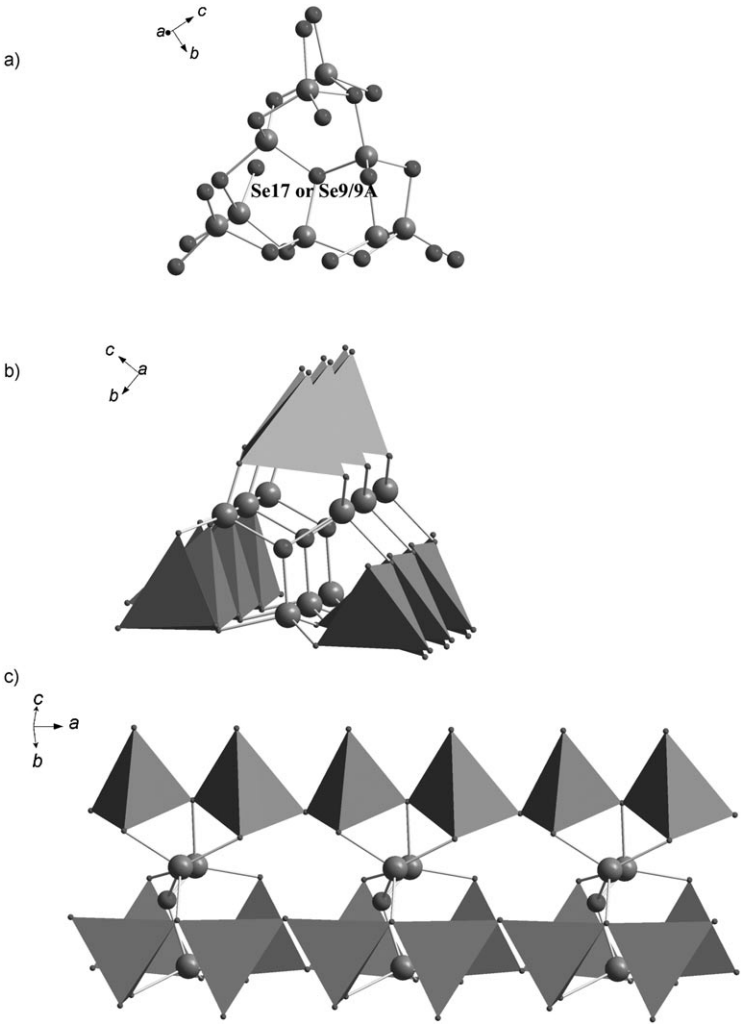

Figure 2. a) The nona-nuclear $[In_9(\mu_3\text{-}Se)_4(\mu_2\text{-}Se)_6Se_{5\times1/2}Se_{5\times1/3}]$ cluster formed by the interconnection, by sharing three corners and three edges, of a trinuclear $[In_3Se(Se_{1/2})_6(Se_{1/3})_3]$ and three binuclear $[In_2Se_{1/3}(Se_{1/2})_6]$ building blocks. The central μ_3-Se is the Se17 atom or the split Se9/Se9A atoms. b) A column formed by the interconnection of nona-nuclear clusters, viewed down the *a* axis; c) A view of this column parallel to *a* axis.

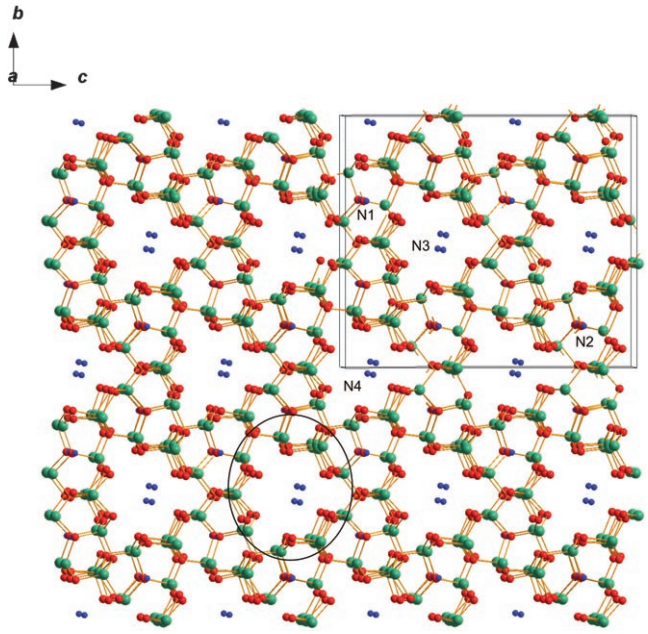

Figure 3. A [100] projection of the three-dimensional framework of **1**. The largest cavities of the structure of **1** filled by $N(3)H_4^+$ and $N(4)H_4^+$ are apparent in this projection. A column of nona-nuclear clusters is highlighted by drawing a circle around it.

To form the 3D-framework, the columns are interconnected, along *b* and *c* axes, by sharing their chains of $InSe_4$ tetrahedra, Figure 3. If the structure is described in terms of clusters, we may consider the connection mode of columns as sharing the binuclear units of their nona-nuclear clusters between them. The columns are arranged in a hexagonal fashion resulting in a honeycomb-type of framework (Figure 3). The three-dimensional framework of **1** exhibits cavities with relatively thick walls and channels running along [100] and [001] directions (Figure 3). Cavities of four different sizes can be found for **1** by using the CAVITY-PLT utility of PLATON.[14] The largest cavities with diameters of 4.4 and 4.2 Å (excluding Van der Waals radii) host ammonium cations N3 and N4, which are positionally disordered in the cage (Figures 3 and 4a). The smallest cavities, which have diameters of 3.4 and 2.7 Å (excluding Van der Waals radii), are located in between the cluster units (**1a**) and host ammonium ions N1 and N2 which are ordered (Figures 3 and 4b). The accessible volume of **1** (or the volume of the void space, not taking into account the NH_4^+) calculated by PLATON is 27% of the total volume of the structure.

To obtain a better understanding of the empty space in **1**, we plotted the isosurface which lies between the framework and the voids (see Figure 5a,b).[15] It is apparent from this plot that the two types of pancake-shaped cavities of com-

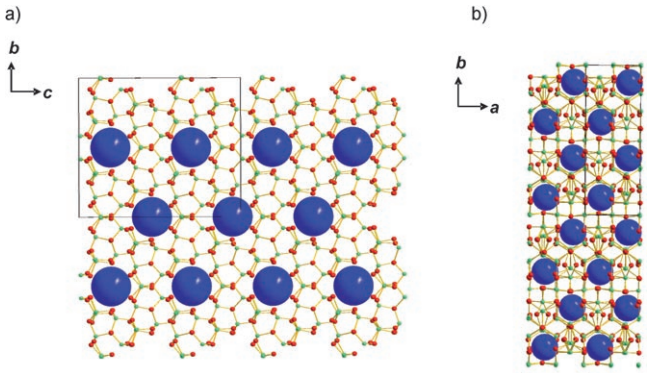

Figure 4. a) A [100] projection of the structure of **1** with the N3 and N4 sites represented by oversized spheres to show the available space around them. The diameters of the cavities hosting N3 and N4 are 4.2–4.4 Å; b) A [001] projection of the same structure with the N1, N2 sites shown as oversized spheres. The diameters of the cavities hosting the N1, N2 atoms are 2.7–3.4 Å.

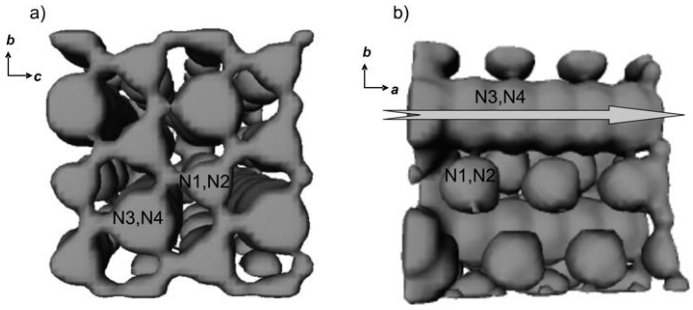

Figure 5. a) Depiction of the void space of the structure of **1** (with labeling of the N1,N2 and N3,N4 cavities) viewed down the *a* axis of the isosurface representing the atom-free space in $In_{12}Se_{20}^{4-}$; b) Depiction of the void space of the same structure (with labeling of the N1/N2 and N3/N4 cavities) viewed down the *c* axis. The possible diffusion of the ions, during the ion-exchange process, through the channels running parallel to *a* axis is indicated by the arrow.

pound **1** (N1, N2 and N3, N4 cavities) communicate forming a three-dimensional tunnel network. The large cavities (N3, N4) actually form 1D channels or columns along *a* axis (Figure 5b). These columns are not connected directly to each other, but they communicate through the small N1, N2 cavities. The diameter of the pore window between the N3, N4 and N1, N2 cavities was estimated at ≈2 Å based on the crystal structure and isosurface plot.

Compound **2** crystallizes in the trigonal space group $R\bar{3}$ and is isostructural with $K_2In_{12}Se_{19}$, which was prepared with conventional solid-state synthesis.[11] More details about the structure of **2** can be found in the Supporting Information.

Ion-exchange capacity of $(NH_4)_4In_{12}Se_{20}$ with alkali metals and H^+: The fact that **1** has a relatively open structure prompted us to study the ion-exchange properties of this compound. Typically, the ion-exchange reactions are complete in few hours at room temperature (see Experimental Section). The results of various ion-exchange experiments are summarized in Table 2. Compound **1** can easily exchange two of its four NH_4^+ ions with K^+, Rb^+, Cs^+, and H^+. All exchanged products exhibit very similar powder X-ray diffraction (PXRD) patterns to that of the pristine material confirming a topotactic ion-exchange mechanism (see, for example, Figure 6a) and implying a robust nature for the framework. The material exhibits selectivity against Na^+ and Li^+; this fact can be explained in terms of the strongly held hydration sphere of Na^+ and Li^+ that prevents the large hydrated ions from entering the structure. Similar selectivity against these alkali cations was also observed for $K_6Sn[Zn_4Sn_4S_{17}]$ and it appears to be a characteristic property of small pore frameworks.[6] This is a useful feature that

Table 1. Crystallographic data for compounds $(NH_4)_4In_{12}Se_{20}$ (**1**) and $(NH_4)_2In_{12}Se_{19}$ (**2**).

	1	**2**
formula	$(NH_4)_4In_{12}Se_{20}$	$(NH_4)_2In_{12}Se_{19}$
M_r	3029.17	2914.133
space group	$Pca2_1$	$R\bar{3}$
a [Å]	8.155(3)	13.8518(6)
b [Å]	22.320(8)	13.8518(6)
c [Å]	25.850(9)	17.6556(16)
V [Å^3]	4750(3)	2933.77(32)
Z	4	3
ρ_{calc}d [g cm^{-3}]	4.253	4.934
μ [mm^{-1}]	21.239	24.612
$2\theta_{max}$ [°]	56.6	58.22
reflections collected	41072	6538
unique reflections (total)	10822	1606
unique reflections [$I>2\sigma(I)$]	6134	904
parameters	331	61
goodness of fit on F^2	1.087	0.789
Flack parameter	0.06(2)	–
final R_1/wR_2 [%]	6.60/12.73	3.54/8.05
largest diff. peak/hole [e A^{-3}]	4.488/−3.212	2.511/−2.294

Table 2. Calculated formulae based on EDS and % H, N analyses for the products of the ion-exchange reactions between **1** and various cations as well as band-gap energies for these materials.

Cation used	EDS formula of the exchanged material	Formula of the exchanged material based on H,N analyses	Band-gap energy [eV]
K^+	complete overlap of K and In peaks	$\mathbf{K_2}(NH_4)_2In_{12}Se_{20}$ calcd (%): H 0.26, N, 0.91; found: H 0.26, N 0.93	2.10
Rb^+	$Rb_2In_{11.3}Se_{20.1}$	$\mathbf{Rb}_2(NH_4)_2In_{12}Se_{20}$ calcd (%): H 0.25; N 0.88; found: H 0.46, N 0.89	2.10
Cs^+	$Cs_{1.4}In_{11.5}Se_{20.4}$	$\mathbf{Cs}_{1.75}$ $(NH_4)_{2.25}$ $In_{12}Se_{20}$ calcd (%): H 0.29, N 0.97; found: H 0.44, N 0.97	2.10
Ag^+	$Ag_{0.9}In_{11.2}Se_{21.5}$	$\mathbf{Ag_{1.3}}(NH_4)_{2.7}In_{12}Se_{20}$ calcd (%): H 0.38, N 1.19; found: H 0.46, N 1.19	1.95
H^+	–	$\mathbf{H_{2.0}}(NH_4)_2In_{12}Se_{20}$ calcd (%): H 0.34, N 0.94; found: H 0.32, N 0.98	1.85
Pb^{2+}	$Pb_{0.5}In_{11.4}Se_{21.4}$	$\mathbf{Pb_{0.65}}(NH_4)_{2.7}In_{12}Se_{20}$ calcd (%): H 0.35, N 1.21; found: H 0.46, N 1.20	2.05
Hg^{2+}	$HgIn_{11.27}Se_{20.9}$	$\mathbf{Hg_{0.6}}(NH_4)_{2.8}In_{12}Se_{20}$ calcd (%): H 0.36, N 1.24; found: H 0.47, N 1.24	1.98

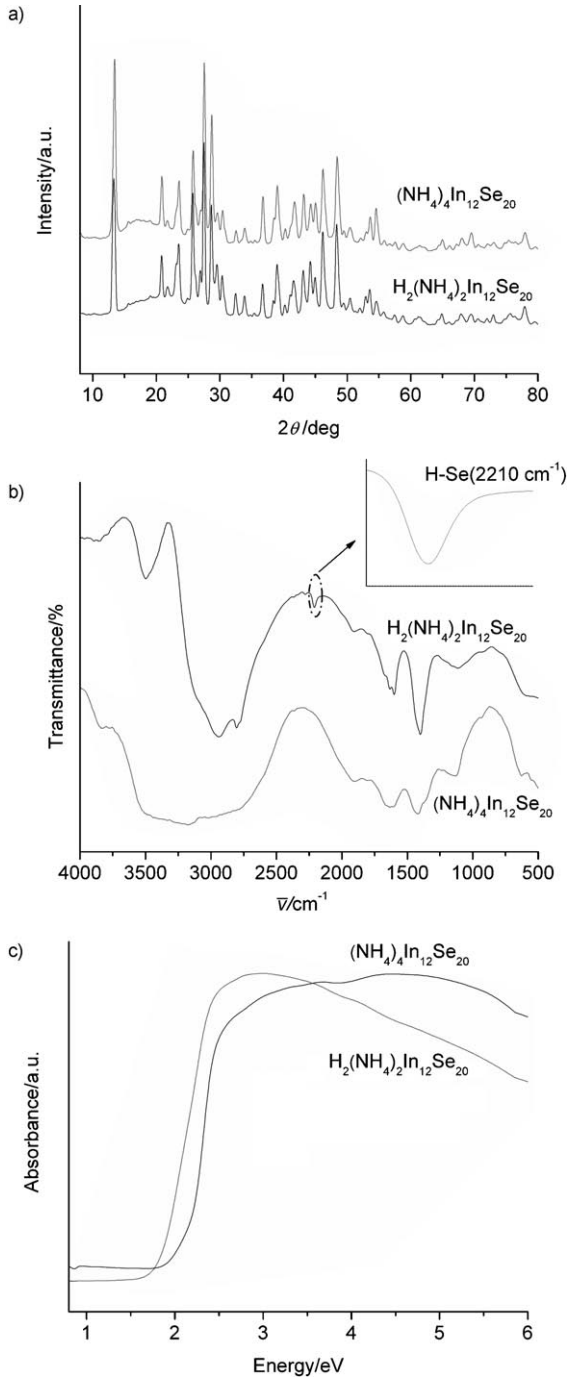

Figure 6. a) PXRD patterns of the pristine $(NH_4)_4In_{12}Se_{20}$ and the proton-exchanged $H_2(NH_4)_2In_{12}Se_{20}$; b) Mid-IR spectrum of the proton-exchanged material $H_2(NH_4)_2In_{12}Se_{20}$ (black line) versus the mid-IR of the pristine $(NH_4)_4In_{12}Se_{20}$. Inset: The peak assigned to H–Se bonds. The absorptions at $\approx$3500 cm^{-1} are due to O–H of H_2O or H_3O^+ and those at $\approx$3000 and 1400 cm^{-1} are assigned to NH_4^+ (see reference [19]); c) Solid-state UV/Vis spectra for the pristine $(NH_4)_4In_{12}Se_{20}$ and the proton-exchanged $H_2(NH_4)_2In_{12}Se_{20}$.

can be exploited in separations for which discrimination against the small alkali cations is desired.

Compound **2** did not show any ion-exchange capacity probably because of its less open structure that results in low mobility of its NH_4^+ counterions.

Explanation of the ion-exchange properties of $(NH_4)_4In_{12}Se_{20}$: The four crystallographically different NH_4^+ ions (disordered in the large cavities and ordered in the small ones) have profoundly different ion-exchange properties. These properties can be understood on the basis of the pore connectivity of the framework of **1**. Specifically, based on the isosurface plot of compound **1** (Figure 5), the pore windows between the N1, N2 and N3, N4 cavities were calculated $\approx$2.0 Å. This size is much smaller than the size of K, Rb^+, Cs^+, and H_3O^+. Thus, the small pores N1, N2 cannot be accessible for these ions during the ion-exchange process. Indeed, the experiments proved a maximum exchange capacity of **1** equal to two equivalents per mole. Presumably, only the N3, N4 cavities hosting the disordered $[N(1)H_4]^+$ and $[N(2)H_4]^+$ ions are involved in the ion-exchange process. The diffusion of the ions is likely to proceed through the 1D channels formed by the N3, N4 cavities along *a* axis (Figure 5b), taking into account that the movement of ions from the N3, N4 to N1, N2 cavities is restricted by the small window between them. Thus, the ion-exchange properties of **1** are controlled by the pore and windows sizes. This is a common situation in ion-exchange materials with rigid three-dimensional frameworks, such as the zeolites.[16] Indeed, the framework of **1** seems to be very rigid, since almost no contraction or expansion in the lattice was observed after the ion-exchange processes. This rigidity is unusual for an open-framework chalcogenide material and is probably due to the thick walls of its cavities.

In general, three-dimensional open-framework chalcogenides are very flexible because 1) are built by corner-sharing or metal-linked clusters and thus, have cavities with relatively thin walls[2,3,6] and 2) the metal-chalcogen-metal angles (100–115°) are relatively small [compared to Al-O-Si angles ($\approx$160–180°) in zeolites], thus allowing expansion of the framework. For example, $K_6Sn[Zn_4Sn_4S_{17}]$, a three-dimensional chalcogenide framework with three different kinds of pores, displays ion-exchange properties that are not consistent with its pore window size and thus, these properties were explained on the basis of a possible "breathing action" of the framework.[6,17]

Heavy-metal-ion-exchange and remediation properties of $(NH_4)_4In_{12}Se_{20}$: Compound **1** showed ion-exchange capacity for heavy-metal ions (like Ag^+, Hg^{2+}, and Pb^{2+}). Ion-exchange reactions employing exactly one equivalent of Ag or 0.5 equivalenst of Hg or Pb yielded almost pure exchanged products. Reactions of **1** with use of more than one equivalent of Ag^+ or more than 0.5 equivalents of Hg^{2+} or Pb^{2+} resulted in partial decomposition of **1** to other phases (possibly binary selenides). Although we could not detect additional phases from the PXRD patterns, solid-state UV/Vis measurements showed at least two different optical band gaps revealing existence of more than one phase for the products of the reactions with $>$one equivalent of Ag^+ or $>$0.5 equivalents of Hg^{2+} or Pb^{2+}.

Removal of heavy-metal ions is of particular interest in the science of purification of the drinking or waste water

from such toxic metal ions.[10] Chalcogenides due to the presence of the chalcogen (S, Se, Te) ligands are expected to be more capable of heavy-metal remediation than oxygen-containing materials like zeolites. Indeed, preliminary investigations of the ability of **1** to clean solutions containing chalcophilic heavy-metal ions, such as Ag^+, Hg^{2+}, and Pb^{2+}, are very encouraging. Compound **1** has been found capable of removing 99.9% of Hg^{2+}, 99.8% of Ag^+, and 94.9% of Pb^{2+} from aqueous solutions of each of these ions. Specifically, ion-exchange of 50 mg of **1** with a 77.8 ppm solution of Hg^{2+} resulted in removal of 77.74 ppm of Hg from this solution (the concentration of Hg after ion-exchange was 0.06 ppm determined by ICP-AES analysis). The distribution coefficient K_d[10c] estimated from these results (see Experimental Section) was 518267 $mL\,g^{-1}$. This value, which is well-comparable with those of most thiol-functionalized silicates[10], reveals the very high affinity of **1** for Hg. In addition, 20 mg of **1** can reduce the concentration of a Ag^+ solution from 31.7 ppm to 0.054 ppm. The corresponding K_d is 586037 $mL\,g^{-1}$, which is also very high, revealing the high affinity of **1** for silver ions.

Compound **1** can also reduce the concentration of Pb^{2+} solution from 93.8 ppm to 4.76 ppm. The K_d value calculated is $\approx$6928 $mL\,g^{-1}$ indicating a lower affinity of the framework for Pb^{2+} ions than Hg^{2+} or Ag^+ ions. More detailed investigations of the heavy-metal remediation properties of **1** including competitive experiments with various heavy-metal concentrations and various pH conditions are in progress.

Acid stability of compounds 1 and 2: The stability of compounds **1** and **2** in acidic solutions is noteworthy. Samples of these compounds stirred with 2.4 M HCl solution under ambient conditions exhibited PXRD patterns very similar with those of the pristine materials (Figure 6a). No loss of crystallinity was observed for the proton-treated materials. Acid stable open-framework compounds with loosely bound cations, like **1**, are highly attractive because of the possibility of producing stable solid acids. N, H analysis for the proton-treated sample of **1** ($H_2(NH_4)_2In_{12}Se_{20}$ (**1b**)) is consistent with the replacement of two NH_4^+ ions by two H^+ ions. A characteristic peak at 2210 cm^{-1} in the mid-IR spectrum of **1b** (Figure 6b) confirmed the existence of H–Se bonds in this material.[18] A proton conductivity study of **1b** will be interesting.

Optical properties of compounds 1 and 2: Compounds **1** and **2** are semiconductors with band-gap energies of 2.10 and 1.80 eV, respectively (consistent with their red and dark red color, respectively). These band gaps lie well in the energy range suitable for photocatalytic applications in the visible light region.[9] Compound **2** is denser than **1** and this can explain the narrower band gap of **2**. For comparison, γ-In_2Se_3, which is a denser phase than **2**, has a band gap of $\approx$1.5 eV.

The band-gap energies of the K, Rb, and Cs-exchanged materials are nearly the same as those of the pristine material. However, the band gap of the proton-exchanged material $H_2(NH_4)_2In_{12}Se_{20}$ is shifted $\approx$0.25 eV to lower energy (1.85 eV) relative to that of the pristine material (Figure 6c). As no contraction of the framework occurred after proton-exchange (see Figure 6a), the red shift in the band gap of the protonated material can be explained on the basis of bonding interactions of the protons with the Se atoms of the framework, which are expected to be stronger than those between the alkali (Rb, Cs) or ammonium ions and the framework selenium ligands.

The silver-, mercury-, and lead-exchanged materials also have slightly lower band gaps than that of the pristine material (Figure S2 in the Supporting Information). Again the explanation of these band-gap shifts is the strong covalent interaction of Ag, Hg, and Pb ions with the Se atoms of the framework. Ag and Hg are expected to interact more strongly with the framework than Pb. Indeed, the Ag and Hg exchanged materials exhibit slightly lower band-gap energies (1.95–1.98 eV) than that of the Pb-exchanged compound (2.05 eV).

Conclusion

Clearly, a hydrothermal synthetic approach at high temperatures (as high as 250 °C) or employing long reaction times favors decomposition of the organic amines to produce novel and robust all-inorganic open-framework chalcogenides, such as **1** and **2**. Although probably hard to control, in principle, the planned decomposition of an organic template at high temperatures can be used as part of a synthetic strategy rather than viewed as an undesirable side reaction. Alternatively, all-inorganic open-framework chalcogenides can be isolated by using concentrated NH_4OH, as we demonstrated for first time in this work.

$(NH_4)_4In_{12}Se_{20}$ (**1**) has a unique structure type and is an uncommon example of an open-framework chalcogenide with thick walls and more rigid network. Compound **1** can replace approximately two of its NH_4^+ ions by two protons, thus yielding a proton-exchanged material, which is a rare example of a solid acid open-framework chalcogenide. The compound showed ion-exchange properties with a series of cations, including a high affinity for soft heavy-metal ions. This highlights the potential of non-oxidic framework solids for functions and reactions that are not suitable or even possible with zeolites or other metal oxides. The capacity of **1** for adsorption of heavy-metal ions from water solutions is very high and comparable with that of mesoporous thiol-functionalized silicates, which are the most efficient adsorbents for heavy-metal ions. A detailed study of the heavy-metal-ion-remediation properties of **1** is underway.

Experimental Section

Materials: In metal was purchased from Cerac. Se, CsCl, RbI, KI, $AgNO_3$, $Hg(NO_3)_2$, $Pb(NO_3)_2$, NH_4OH (28–30% in H_2O) and dipropylamine (DPA) were purchased from Aldrich.

Synthesis of $(NH_4)_4In_{12}Se_{20}$ (1)

Method A: Elemental In (3.4 mmol) and Se (4.8 mmol), water (10 mL), and DPA (4.8 mmol) were mixed in a 23 mL Teflon-lined stainless steel autoclave. The autoclave was sealed and placed in a box furnace with a temperature of 190 °C. The autoclave remained undisturbed at this temperature for three weeks. Then, the autoclave was allowed to cool at room temperature. The red rodlike crystals of **1** were isolated by filtration (yield ≈89% based on In), washed several times with water, acetone, and diethyl ether (in this order) and dried in air. A very small quantity of dark red polyhedral-shaped crystals of **2** coexisted in the product. However, the crystals of **1** could be manually separated from those of **2**. The purity (>95%) of the product was confirmed by PXRD measurements. Elemental analysis calcd (%) for $H_{16}In_{12}N_4Se_{20}$ (3029.17): C 0, H 0.54, N 1.75; found: C 0.11, H 0.53, N 1.84.

Method B: Elemental In (3.4 mmol) and Se (4.8 mmol) and concentrated NH_4OH (6 mL, 28–30% in water) were mixed in a 23 mL Teflon-lined stainless steel autoclave. The autoclave was sealed and then placed in a computer-controlled box furnace and heated (≈50 °C h^{-1}) to 250 °C for 48 h, followed by cooling to room temperature at 50 °C h^{-1}. The crystals of **1** were isolated by filtration (yield ≈70% based on In), washed several times with water, acetone, and diethyl ether (in this order) and dried in the air. The small quantities of unreacted In and Se were manually separated from the red crystals of **1**. The purity (>95%) of the product was confirmed by PXRD measurements. Elemental analysis calcd (%) for $H_{16}In_{12}N_4Se_{20}$ (3029.17): C 0, H 0.54, N 1.75; found: C 0.14, H 0.50, N 1.65.

Synthesis of $(NH_4)_2In_{12}Se_{19}$ (2): In a typical preparation of **2**, elemental In (3.4 mmol) and Se (8.5 mmol), water (10 mL) and DPA (4.8 mmol) were mixed in a 23 mL Teflon-lined stainless steel autoclave. The autoclave was sealed and then placed in a computer-controlled box furnace and heated (≈50 °C h^{-1}) to 250 °C for 24 h, followed by cooling to room temperature at 50 °C h^{-1}. Then, the dark red crystals of **2** were isolated by filtration (yield 85% based on In), washed several times with water, acetone, and diethyl ether, and dried in air. The purity (>95%) of the product was confirmed by PXRD. Elemental analysis calcd (%) for $H_8In_{12}N_2Se_{19}$ (2914.13): C 0, H 0.27, N 0.96; found: C 0.2; H 0.33; N 0.88.

Ion-exchange experiments with $(NH_4)_4In_{12}Se_{20}$: A typical ion-exchange experiment of **1** with an alkali cation A^+ (A = K^+, Rb^+, Cs^+) was as follows: In a suspension of compound **1** (0.02 mmol) in water (20 mL), excess of AI (0.7 mmol) was added as a solid. The mixture was kept under magnetic stirring for ≈12 h. Then, the red polycrystalline material was isolated by filtration, washed several times with water, acetone, and diethyl ether and dried in the air. Similar experimental routes were followed for the ion-exchange of **1** with H^+, Hg^{2+}, Ag^+, and Pb^{2+}.

Powder X-ray diffraction (PXRD): The samples were examined by X-ray powder diffraction for identification and to assess phase purity. Powder patterns were obtained using a CPS 120 INEL X-ray powder diffractometer with Ni-filtered $Cu_{K\alpha}$ radiation operating at 40 kV and 20 mA and equipped with a position-sensitive detector. Samples were ground and spread on a glass slide. The purity of phases was confirmed by comparison of the X-ray powder diffraction patterns to ones calculated from single crystal data using the NIST Visualize 1.0.1.2 software.

Energy dispersive spectroscopy (EDS) analyses: The analyses were performed with a JEOL JSM-6400 V scanning electron microscope (SEM) equipped with a Tracor Northern energy dispersive spectroscopy (EDS) detector. Data acquisition was performed with an accelerating voltage of 25 kV and 40 s accumulation time.

ICP-AES (inductively coupled plasma atomic emission spectroscopy) analyses: The concentrations of the Ag^+, Hg^{2+}, and Pb^{2+} ions of the solutions after the ion-exchange processes were determined by ICP-AES by using a VISTA AX CCD instrument. The ICP-AES intensity was the result of three (30 s) exposures. For each sample, four readings of the ICP-AES intensity were recorded and averaged. One standard was reanalyzed after analysis of the samples. The measurements were performed by the Toxicology Laboratory at Animal Health and Diagnostic Center of Michigan State University.

Calculation of the distribution coefficient K_d (mL g^{-1}): The distribution coefficient K_d is given by the equation $K_d = [(C_0 - C_f)/C_f](V/m)$, in which C_0 and C_f are the initial and equilibrium concentration of Hg^{2+} (ppm), V is the volume (mL) of the testing solution, and m is the amount of the ion exchanger (g) used in the experiment.[10c]

IR spectroscopy: Fourier transform infrared spectra (FT-IR) in the mid-IR region [4000–600 cm^{-1}, diffuse reflectance infrared Fourier transform (DRIFT) method] were recorded with a computer-controlled Nicolet 750 Magna-IR series II spectrometer equipped with a TGS/PE detector and silicon beam splitter in 2 cm^{-1} resolution.

Solid-state reflectance UV/Vis/Near IR spectroscopy: UV/Vis/Near-IR diffuse reflectance spectra were obtained at room temperature on a Shimadzu UV-3010 PC double beam, double monochromator spectrophotometer in the wavelength range of 200–2500 nm. $BaSO_4$ powder was used as a reference (100% reflectance) and base material on which the powder sample was coated. The reflectance data were converted to absorption using the Kubelka–Munk function, and the band edge for each sample was estimated from the intercept of the line extrapolated from the high-energy end of the absorption to the baseline.

C, H, N analyses: Elemental C, H, N analyses were obtained on a Perkin-Elmer Series II CHNS/O Analyzer 2400.

Single-crystal X-ray crystallography: A Siemens SMART Platform CCD diffractometer operating at room temperature and using graphite-monochromatized $Mo_{K\alpha}$ radiation was used for data collection. Cell refinement and data reduction were carried out with the program SAINT.[19] An empirical absorption correction was done to the data using SADABS.[19] The space group for structure of **1** was determined from systematic absences and intensities were extracted by the program XPREP.[20] The atom Se9 of the structure of **1** was modeled as a split site. Attempts to solve the structure with a super-cell model have not been successful so far. For the structure of **2** a twin law (−1 −1 0 0 1 0 0 0 −1) was applied, suggested by the TWINROTMAT utility of PLATON.[13] This reduced the R value from ≈35.6% to 17.5%. Further reduction of the R value to 5.0% was achieved by applying the split site model for In2 and In3 atoms (the final R value of 3.54% was obtained after the anisotropic refinement). The structures were solved with direct methods by using SHELXS and least-squares refinement was done against F^2 by using routines from SHELXTL software.[20] Selected crystal data for the structures of compounds **1** and **2** are given in Table 1. Further details on the crystal structure investigations may be obtained from the Fachinformationszentrum Karlsruhe, 76344 Eggenstein-Leopoldshafen, Germany (fax: (+49) 7247-808-666; e-mail: crysdata@fiz-karlsruhe.de), on quoting the depository numbers CSD-41729 and -41730. See also the Supporting Information.

Acknowledgements

Financial support from the National Science Foundation (DMR-0443785 and CHE-0211029 Chemistry Research Group) is gratefully acknowledged.

[1] a) S. Dhingra and M. G. Kanatzidis, *Science* **1992**, *258*, 1769; b) T. J. McCarthy, T. A. Tanzer, M. G. Kanatzidis, *J. Am. Chem. Soc.* **1995**, *117*, 1294; c) G. A. Marking, M. G. Kanatzidis, *Chem. Mater.* **1995**, *7*, 1616; d) E. A. Axtel III, M. G. Kanatzidis, *Chem. Mater.* **1996**, *8*, 1350; e) J. A. Hanko, M. G. Kanatzidis, *Angew. Chem.* **1998**, *110*, 354; *Angew. Chem. Int. Ed.* **1998**, *37*, 342; f) Enos A. Axtell III, Y. Park, K. Chondroudis, M. G. Kanatzidis, *J. Am. Chem. Soc.* **1998**, *120*, 124; g) C. L. Cahill, J. B. Parise, *Dalton Trans.* **2000**, 1475; h) Y. Ko, C. L. Cahill, J. B. Parise, *Chem. Commun.* **1994**, 69; i) C. L. Cahill, Y. Ko, J. B. Parise, *Chem. Mater.* **1998**, *10*, 19; j) C. L. Cahill, B. Gugliotta, J. B. Parise, *Chem. Commun.* **1998**, 1715; k) C. L. Bowes, G. A. Ozin, *Adv. Mater.* **1996**, *8*, 13, and references therein; l) W. S. Sheldrick, M. Wachhold, *Angew. Chem.* **1997**, *109*, 214; *Angew. Chem. Int. Ed. Engl.* **1997**, *36*, 206, and references therein. m) K. Chondroudis, M. G. Kanatzidis, *J. Solid State Chem.* **1998**, *136*, 328.

[2] a) H. Li, A. Laine, M. O'Keefe, O. M. Yaghi, *Science* **1999**, *283*, 1145; b) H. Li, J Kim, T. L. Groy, M. O'Keefe, O. M. Yaghi, *J. Am.*

Chem. Soc. **2001**, *123*, 4867; c) H. Li, J Kim, M. O'Keefe, O. M. Yaghi, *Angew. Chem.* **2003**, *115*, 1817; *Angew. Chem. Int. Ed.* **2003**, *42*, 1819; d) O. M. Yaghi, Z. Sun, D. A. Richardson, T. L. Groy, *J. Am. Chem. Soc.* **1994**, *116*, 807.

[3] a) P. Feng, X. Bu, N. Zheng, *Acc. Chem. Res.* **2005**, *38*, 293; b) X. Bu, N. Zheng, P. Feng, *Chem. Eur. J.* **2004**, *10*, 3356, and references therein; c) N. Zheng, X. Bu, P. Feng, *Angew. Chem.* **2004**, *116*, 4857; *Angew. Chem. Int. Ed.* **2004**, *43*, 4753; d) N. Zheng, X. Bu, P. Feng, *Nature* **2003**, *426*, 428; e) N. Zheng, X. Bu, P. Feng, *J. Am. Chem. Soc.* **2005**, *127*, 5286; f) X. Bu, N. Zheng, Y. Li, P. Feng, *J. Am. Chem. Soc.* **2003**, *125*, 6024; g) N. Zheng, X. Bu, B. Wang, P. Feng, *Science* **2002**, *298*, 2366; h) C. Wang, X. Bu, N. Zheng, P. Feng, *J. Am. Chem. Soc.* **2002**, *124*, 10268.

[4] a) X. Huang, J. Li,, H. Fu, *J. Am. Chem. Soc.* **2000**, *122*, 8789; b) X. Chen, X. Huang, A. Fu, J. Li, L.-D. Zhang, H.-Y. Guo, *Chem. Mater.* **2000**, *12*, 2385; c) W. Su, X. Huang, J. Li, H. Fu, *J. Am. Chem. Soc.* **2002**, *124*, 12944.

[5] a) N. Ding, D-.Y. Chung, M. G. Kanatzidis, *Chem. Commun.* **2004**, 1170; b) N. Ding, M. G. Kanatzidis, *Angew. Chem.* **2006**, *118*, 1425; *Angew. Chem. Int. Ed.* **2006**, *45*, 1397.

[6] M. J. Manos, R. G. Iyer, E. Quarez, J. H. Liao, M. G. Kanatzidis, *Angew. Chem.* **2005**, *117*, 3618; *Angew. Chem. Int. Ed.* **2005**, *44*, 3552.

[7] a) S. H. Jhung, J. W. Yoon, J.-S. Hwang, A. K. Cheetham, J.-S. Chang, *Chem. Mater.* **2005**, *17*, 4455; b) S. H. Jhung, J.-S. Chang, S.-E. Park, P. M. Forster, G. Férey, A. K. Cheetham, *Chem. Mater.* **2004**, *16*, 1394.

[8] The only known examples of open-framework indium selenides hydrothermally synthesized are reported in the following papers: a) C. Wang, X. Bu, N. Zheng, P. Feng, *Angew. Chem.* **2002**, *114*, 2039; *Angew. Chem. Int. Ed.* **2002**, *41*, 1959; b) C. Wang, X. Bu, N. Zheng, P. Feng, *Chem. Commun.* **2002**, *13*, 1344.

[9] N. Zheng, X. Bu, H. Vu, P. Feng, *Angew. Chem.* **2005**, *117*, 5433; *Angew. Chem. Int. Ed.* **2005**, *44*, 5299.

[10] a) X. Feng, G. E. Fryxell, L.-Q. Wang, A. Y. Kim, J. Liu, K. M. Kemner, *Science* **1997**, *276*, 923; b) L. Mercier, T. J. Pinnavaia, *Adv. Mater.* **1997**, *9*, 500; c) C. Liu, Y. Huang, N. Naismith, J. Economy, *Environ. Sci. Technol.* **2003**, *37*, 4261; d) L. Zhang, W. Zhang, J. Shi, Z. Hua, Y. Li, J. Yan, *Chem. Commun.* **2003**, 210; e) J. Liu, X. Feng, G. E. Fryxell, L.-Q. Wang, A. Y. Kim, M. Gong, *Adv. Mater.* **1998**, *10*, 161.

[11] a) M. Schlosser, C. Reiner, H-.J. Deiseroth, L. Kienle, *Eur. J. Inorg. Chem.* **2001**, 2241; b) L. Kienle, A. Simon, *J. Solid State Chem.* **2001**, *161*, 385.

[12] The mesostructured *c*-C_{20}PyPtSnSe material has also shown remarkable acid stability: P. N. Trikalitis, N. Ding, C. Malliakas, S. J. L. Billinge, M. G. Kanatzidis, *J. Am. Chem. Soc.* **2004**, *126*, 15326.

[13] X. Bu, P. Feng, T. E. Gier, G. D. Stucky, *Zeolites* **1997**, *19*, 200.

[14] a) A. L. Spek (2005) PLATON, A Multipurpose Crystallographic Tool, Utrecht University, Utrecht, The Netherlands; b) A. L. Spek, *J. Appl. Crystallogr.* **2003**, *36*, 7–13.

[15] To plot the isosurface, the following parameters were used: 27 unit cells ($3\times3\times3$), resolution = 40, expansion factor = 0.5, smoothing number = 2, boundary condition = 0. The distance corresponding to the 255 value (the maximum distance of a grid point from the Van der Walls sphere) was calculated ≈5.6 Å. Based on this value, the diameter of the largest cavity (N3, N4) was estimated ≈5.0 Å and that of the smallest cavity (N1, N2) was found ≈2.8 Å. The volume of the empty space was found 30.6% of the total volume. These values for the accessible volume and the diameters of the cavities are in good agreement with those calculated by PLATON (see text). The calculation of the diameters of windows connecting the pores was done based on the values (given by the isosurface program) for which the overlap between these pores is minimum. Estimation of the pore windows can be done only by the program that we have used for plotting the isosurface and not by PLATON. More details about this program are given in the following reference: T. F. Nagy, S. D. Mahanti, J. L. Dye, *Zeolites* **1997**, *19*, 57.

[16] a) Y. Watanabe, H, Yamada, J. Tanaka, Y. Komatsu, Y. Moriyoshi, *Sep. Sci. Technol.* **2004**, *39*, 2091; b) Y. Watanabe, H. Yamada, H. Kokusen, J. Tanaka, Y. Moriyoshi, Y. Komatsu, *Sep. Sci. Technol.* **2003**, *38*, 1518; c) H. S. Sherry, *J. Phys. Chem.* **1966**, *70*, 1158.

[17] M. J. Manos, K. Chrissafis, M. G. Kanatzidis, *J. Am. Chem. Soc.* **2006**, *128*, 8885.

[18] V. Riede, H. Neumann, H. Sobotta, C. Ascheron, B. V. Novikov, *Solid State Commun.* **1987**, *61*, 113.

[19] K. Nakamoto, in *Infrared and Raman Spectra of Inorganic and Coordination Compounds*, 3rd ed, Wiley, **1977**; for a discussion of NH_4^+, H_2O and H_3O^+ vibrational frequencies see p. 135, pp. 226–230 and pp. 119–122, respectively.

[20] Siemens Analytical X-Ray Instruments Inc., **1995**.

[21] G. M. Sheldrick, SHELXTL, Crystallographic Software Package, SHELXTL, Version 5.1, Bruker-AXS, Madison, WI, **1998**.

Received: June 22, 2006
Revised: October 7, 2006
Published online: November 22, 2006

